

Reversible Swarming and Separation of Self-propelled Chemically-Powered Nanomotors under Acoustic Fields

Tailin Xu^{1,2}, Fernando Soto¹, Wei Gao¹, Renfeng Dong¹, Victor Garcia-Gradilla¹, Ernesto Magaña¹, Xueji Zhang², Joseph Wang^{1*}

¹Department of Nanoengineering, University of California-San Diego, La Jolla, California, 92093, USA

²Research Center for Bioengineering and Sensing Technology, University of Science and Technology Beijing, Beijing 100083, P. R. China

*Address correspondence to josephwang@ucsd.edu

Supporting Videos

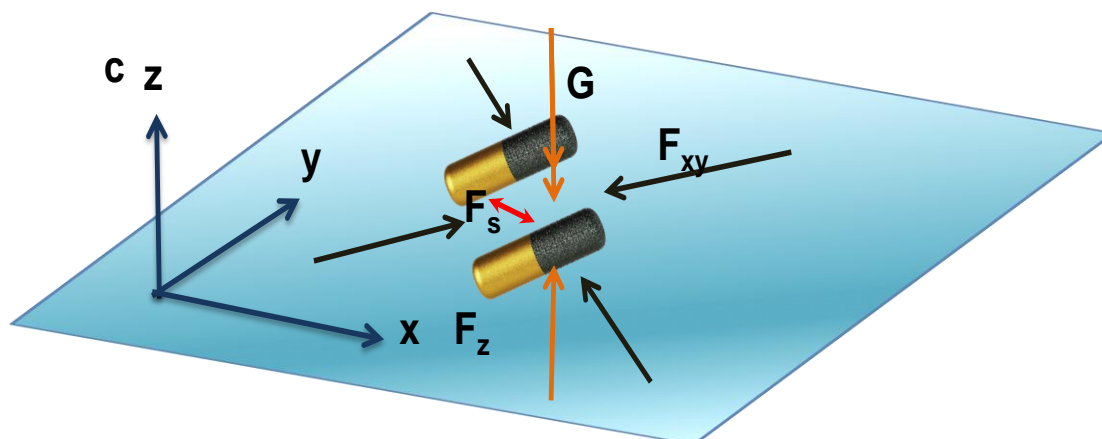
SI Video 1. Catalytic nanomotor swarm formation under acoustic field.

SI Video 2. Ultrasound-triggered reversible swarming and dispersion of Pt-Au catalytic nanowire motors.

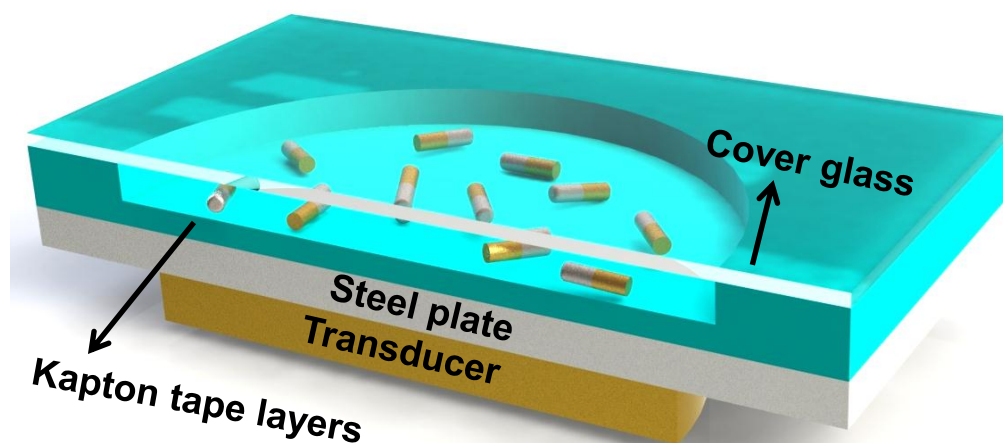
SI Video 3. Transportation of nanomotor swarm by varying the applied frequency.

SI Video 4. Ultrasound induced swarming and separation of Janus spherical motors and Au-Pt nanowire motors.

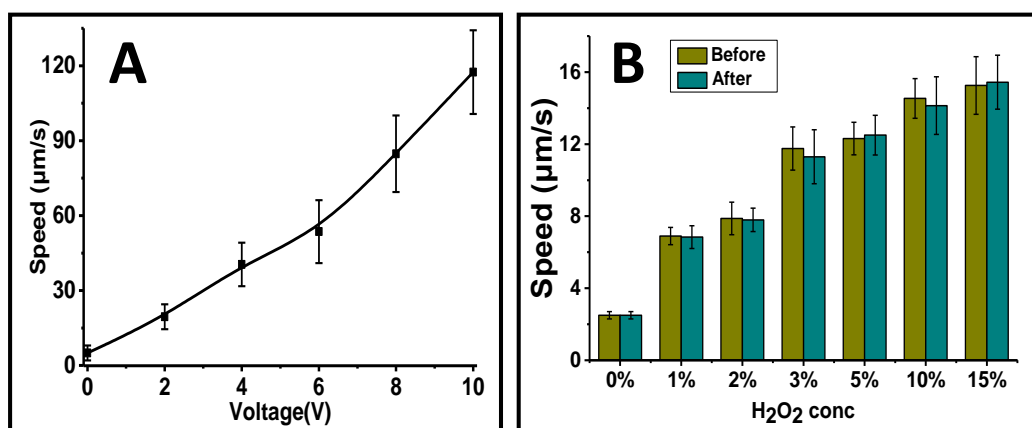
Supporting Figures



SI Figure 1. Schematic illustrating the acoustic radiation forces acting on the nanomotor. The acoustic force can be divided into the primary radiation force (axial component (F_z) and a transverse component (F_{xy}) and the secondary radiation force (F_s); G is the gravity force; other forces such as the hydrodynamic force, the electrostatic force and the van der Waals forces are much smaller (not shown in the paper).



SI Figure 2. Schematic of acoustic cell setup: the PZ26 piezoelectric transducer was attached to the bottom center of a steel plate, with a sample reservoir mounted on top made of Kapton tape layers. A glass slide was used on top as an acoustic reflector.



SI Figure 3. Variables affecting the swarm formation and dispersion of the Au-Pt nanomotor swarm, A) Average speed of swarm formation is dependent upon the applied voltage from 0 to 10 Vpp and the speed measured by average speed of start point to the node. B) Dependence of the motor speed on the hydrogen peroxide fuel concentration before and after the ultrasound-induced swarming. Ultrasound field: applied voltage, 10 Vpp, frequency, 618 KHz.

SI Table 1. Swarming methods and corresponding swarming times reported for different synthetic microparticles.

Type	Method /Trigger	Assembly Time	Dispersion Time	Ref
AgCl particles	UV Light	1.5 min	NA	4
SiO ₂ /TiO ₂ particles	Janus UV Light	0.5 min	0.5 min	5
Ir/SiO ₂ Janus particles	N ₂ H ₄	4 min	NA	6
Au microparticles	N ₂ H ₄ , H ₂ O ₂	1 min	20 min	7
Ag ₃ PO ₄ particles	UV and NH ₃	7 min	7 min	8
Nematic liquid crystal	UV light, Electric	4 min	NA	9
Ti/Cr/Pt microtube engines	H ₂ O ₂	Several seconds	NA	10
AgCl micromotors	UV, H ₂ O ₂	15 min	NA	11
Au-Pt nanowires	Ultrasound	2 s	5 s	This work

SI Table 2. Physical properties of Au-Pt wires Janus particles and water at 25 °C, 1 atm.

	Au-Pt wires	Janus particles	Distilled water
Density (g/cm ³)	20.5 ^a	1.1	0.997
Sound speed (m/s)	2306 ^b	2160	1497
Compressibility (Pa ⁻¹)	9.17x10 ⁻¹²	2.24x10 ⁻¹⁰	4.48x10 ⁻¹⁰
Particle diameter (μm)	R=0.1, L=2	R=0.605	
Viscosity (Pa•s)			1.002x10 ⁻³

^a average density of Au (19.6g/cm³) and Pt (21.4 g/cm³). ^b calculated using the Newton-Laplace equation $U = \frac{1}{\sqrt{\rho\beta}}$

Ultrasound drag force and the catalytic force

The nanomotors remain assembled as long as the acoustic field is applied, indicating that the acoustic forces are significantly larger than the catalytic propulsion force. A drag force of 0.065 pN can be estimated for an electrophoretically-propelled nanowire motor based on Stokes' drag theory:¹²

$$F_d = \frac{2\pi\mu L}{\ln\left(\frac{2L}{R}\right) - 0.7}$$

where μ is the viscosity of the fluid, v is the velocity of the nanomotor, and R and L are the radius and length of the nanowires, respectively. The acoustic force acting on the nanomotors, 0.498 pN, is ~7.7 times larger than the force resulting from the electrophoretic propulsion (0.065 pN). (The acoustic force was calculated based on the speed of the nanomotors movement towards the nodes and using the equation) Such large difference between the forces indicates that the acoustic radiation is the dominant force acting on the nanomotors, thus maintaining the swarm intact.

Experimental Section

All controlled-potential experiments were performed with a CHI 660D potentiostat (CH Instruments, Austin, TX). A Nikon Eclipse 80i microscope, coupled with a 10x and 20x objective, a Photometrics Cool Snap HQ2 CCD camera, and MetaMorph 7.6 software (Molecular Devices, Sunnyvale, CA) were used for capturing videos at 10 frames per second.

Synthesis of catalytic microengines

The Au-Pt nanomotors were prepared by sequential electrodeposition of gold and platinum into 200 nm diameter nanopores of a 60 μm thick alumina membrane template (Catalog No. 6809-6022; Whatman, Maidstone, U.K.). First, a thin gold film was sputtered on the branched side of the membrane to serve as a working electrode. The membrane was assembled in a Teflon plating cell with aluminum foil serving as an electrical contact for the subsequent electrodeposition. A sacrificial copper layer was electrodeposited into the branched area of the membrane using a 1 M cupric sulfate pentahydrate solution ($\text{CuSO}_4 \cdot 5\text{H}_2\text{O}$; Sigma-Aldrich, St. Louis, MO), using a charge of 10 C and a potential of -1.0 V (vs. Ag/AgCl reference electrode) along with platinum wire as a counter electrode. Subsequently, Au segment was plated using a gold plating solution (Orotemp 24 RTU RACK; Technic Inc., Anaheim, CA) a total charge of 1.5 C and a potential of -0.9 V. Platinum was then deposited galvanostatically using a current of -2 mA for 50 min from a platinum plating solution (Platinum RTP; Technic Inc). The resulting Au-Pt nanowires had a length of around 2 μm . The sputtered gold layer and the copper sacrificial layer were simultaneously removed by mechanical polishing using cotton tip applicators soaked with 0.5 M CuCl_2 solution in 20% HCl. The nanomotors were then released by immersing the membrane in 3 M NaOH for 30 min. The resulting nanomotors were separated from solution by centrifugation at 10,000 rpm for 5 min and washed repeatedly with ultrapure water (18.2 M Ω cm) until a neutral pH was achieved. Between washing steps the nanomotors solution was mixed with ultrapure water and briefly sonicated (2-5 seconds) to ensure complete dispersion of nanomotors in the washing water. All nanomotors were stored in ultrapure water at room temperature and their speed was tested before each experiment. Janus particle micromotors were prepared using polystyrene (PS) microparticles (1.21 μm mean diameter, Bangs Laboratories, Fishers, IN, USA) as base particles. First, 20 μL PS particle solution was dispersed into ethyl alcohol (A407-4, Fisher, Pittsburgh, PA, USA) and centrifuged. Then, the PS particles were re-dispersed in 200 μL ethyl alcohol. The sample was then spread onto glass slides and dried uniformly to form particle monolayers. The particles were sputter-coated with a 20 nm Pt layer using the Denton Discovery 18 unit. The deposition was performed at room temperature with a DC power of 200 W and an Ar pressure of 2.5 mT for 15 s. In order to obtain a uniform Janus half-shell coating, rotation was turned off and the sample slides were set up at an angle to be parallel to the Pt target. After the fabrication, the Janus particles were detached from the substrate via sonication or pipette pumping.

Ultrasound equipment

The ultrasonic experiments were carried out in a cell similar to that described

previously.¹⁻³ The cell was made in a steel plate (50 mm x 50 mm x 0.94 mm) with a 240 μm Kapton tape as a protective layer, and a sample reservoir at the center (1 mm), covered by a 18 mm x 18 mm x 0.15 mm glass slide for ultrasound reflection. The piezoelectric transducer which produces the ultrasound waves (Ferropem PZ26 disk 10 mm diameter, 0.5 mm thickness) was attached to the bottom center of the slide by conductive epoxy glue. The continuous ultrasound sine wave was applied via a piezoelectric transducer, through an Agilent 15 MHz arbitrary waveform generator, in connection to a home-made power amplifier. The applied continuous sine waveform had varied frequency and voltage amplitude ranging between 500 and 1000 kHz and from 0 to 10.0 V, respectively, as desired for controlling the intensity of the ultrasonic wave. The electrical signal was monitored using a 20 MHz Tektronix 434 storage oscilloscope.

References

- (1) Xu, T.; Soto, F.; Gao, W.; Garcia-Gradilla, V.; Li, J.; Zhang, X.; Wang, J. *J. Am. Chem. Soc.* **2014**, *136*, 8552.
- (2) Wang, W.; Castro, L. A.; Hoyos, M.; Mallouk, T. E. *ACS Nano* **2012**, *6*, 6122.
- (3) Garcia-Gradilla, V.; Orozco, J.; Sattayasamitsathit, S.; Soto, F.; Kuralay, F.; Pourazary, A.; Katzenberg, A.; Gao, W.; Shen, Y.; Wang, J. *ACS Nano* **2013**, *7*, 9232.
- (4) Ibele, M.; Mallouk, T. E.; Sen, A. *Angew. Chem. Int. Ed. Engl.* **2009**, *48*, 3308.
- (5) Hong, Y.; Diaz, M.; Cordova-Figueroa, U. M.; Sen, A. *Adv. Funct. Mater.* **2010**, *20*, 1568.
- (6) Gao, W.; Pei, A.; Dong, R.; Wang, J. *J. Am. Chem. Soc.* **2014**, *136*, 2276.
- (7) Kagan, D.; Balasubramanian, S.; Wang, J. *Angew. Chem. Int. Ed.* **2011**, *50*, 503.
- (8) Duan, W.; Liu, R.; Sen, A. *J. Am. Chem. Soc.* **2013**, *135*, 1280.
- (9) Hernández-Navarro, S.; Tierno, P.; Farrera, J. A.; Ignés-Mullol, J.; Sagués, F. *Angew. Chem. Int. Ed.* **2014**, *126*, 10872.
- (10) Solovey, A. A.; Mei, Y.; Schmidt, O. G. *Adv. Mater.* **2010**, *22*, 4340.
- (11) Ibele, M. E.; Lammert, P. E.; Crespi, V. H.; Sen, A. *ACS Nano* **2010**, *4*, 4845.
- (12) Happel, J.; Brenner, H. *Low Reynolds number hydrodynamics*; Springer Netherlands, **1983**.